

# Application of Functional Polyhedral Oligomeric Silsesquioxane Reinforced Poly(lactic acid) Nanocomposites in Biomedicine

Jiaming Lin <sup>1,&</sup>, Weidong Gan <sup>1,&</sup>, Anfei Huang <sup>1</sup>, Bata Wang <sup>1</sup>, Lin Zhou <sup>2,\*</sup>, Yongxin Lin <sup>2,\*</sup>

<sup>1</sup> The First Clinical Medical College of Jinan University, Guangzhou, China

<sup>2</sup> Department of Orthopedic, The First Affiliated Hospital of Jinan University, Guangzhou, China

<sup>&</sup> These authors contributed to the work equally and should be regarded as co-first authors

\* Correspondence: hyzhoulin@126.com (L.Z.); linyongxin512@aliyun.com (Y.L.)

**Abstract:** Polylactic acid (PLLA), a biodegradable aliphatic polyester, has been widely used in biomedical applications. However, some existing shortcomings limit its widespread use in biological materials such as relatively insufficient crystallinity, low thermal stability and excessive brittleness. Incorporating POSS nanoparticles into PLLA can overcome the above disadvantages. In our previous study, a series of octahedral oligomeric silsesquioxanes POSS-(PLLA)<sub>8</sub> were prepared to pull into the PLLA tail into the POSS particles and the interfacial interaction between PLLA and POSS, those would improve the mechanics and biocompatibility of PLLA. In this article, the POSS nanoparticles POSS-(PLLA)<sub>32</sub> with 32 PLLA tail chains were compared with POSS-(PLLA)<sub>8</sub> nanofibers, and this study was systematically investigated the effects of tail length on the biological properties of nanocomposite fibers. The fiber of POSS-(PLLA)<sub>8</sub> composite nanofiber has a relatively good uniform distribution and a regular porous structure with a diameter of 300-700 nm. From the FESEM chart, the POSS-(PLLA)<sub>8</sub> nanoparticles have good dispersibility, and no serious agglomeration occurs on the surface of the composite fiber. Compared with pure PLLA nanofibers, the adjunction of POSS-PLLA<sub>8</sub> introduce a large number of relatively regular and small size wafers, which form the most compact and largest number of crystals and improve the thermal stability and hydrophilic properties of PLLA/(POSS-(PLLA)<sub>8</sub> composite nanofibers. The (POSS-(PLLA)<sub>8</sub> nanoparticles are introduced into the PLLA matrix material, and the nanoparticles act as a heterogeneous nucleating agent, which greatly increases the crystallinity of the system, and the composite material has a smaller size and a more regular crystal form. The strength of the composite material has been greatly improved. On the other hand, the incorporation of (POSS-(PLLA)<sub>8</sub> nanoparticles can effectively promote the interaction of the interface and improve the interfacial compatibility. In addition, PLLA/(POSS-(PLLA)<sub>8</sub> composite porous nanofibers can promote cell proliferation, spreading and adhesion, and have good biocompatibility.

**Keywords:** nanocomposite; polyhedral oligomeric silsesquioxane; poly(L-lactic acid); mechanical properties; biocompatibility

## 1. Introduction

Organic-inorganic hybrid polymers are promising functional materials and have been used in many different fields, which mainly including catalysis, sensing, drug delivery and biotechnology [1,2]. It consists of a nanoscale inorganic material as a core (consisting of alternating Si-O-Si bonds) and an organic material as a shell [3]. This makes the external organic molecular group diverse, and it also has considerable functionality and performance designability [4].

Generally, POSS-based polymer nanocomposites can be classified into four categories based on the combination of the groups participating in the reaction and the polymer composite: (a) Functional POSS as a mixed material with a non-reactive group incorporated into the polymer; (b) Focusing on functionalized POSS, it is playing a role on a microinitiator that initiates polymerization between POSS and the polymer matrix; (c) POSS with a monofunctional group acts as a binding macromolecule through a grafting reaction and binds to a macromolecular skeleton; (d) Multifunctional POSS as a nanofiller for modified polymer matrix [4-6]. Based on the above four methods for preparing polymer-POSS composites, the mechanical, thermal, optical, and crystallization properties of the polymer matrix can be significantly improved [7,8]. For example, by introducing functionalized 1, 2-propanediol isobutyl POSS (PHI-POSS) as a pendant group, octahydroxy POSS (OCTA-POSS) chemical crosslinker can improve the thermal stability and flammability of rigid polyurethane foams [9]. Hybrid polystyrene (PS) prepared by a simple Friedel-Crafts reaction from a single vinyl-substituted POSS and PS has better solubility, crystallinity and thermal properties [10]. The properties of nanocomposites depend not only on the overall properties of each component, but also on the complex interactions

between them. The major challenge in current research of POSS nanomaterials is remaining the uniform dispersion of the polymer matrix.

Poly(lactic acid) (PLLA), a biodegradable aliphatic polyester, has been widely used in biomedical applications, including Drug carrier system [11,12], tissue engineering scaffold material [13-15], the raw material of surgical suture [16,17], artificial blood vessel [18,19]. However, some existing shortcomings limit its widespread use in biological materials such as relatively insufficient crystallinity, low thermal stability and excessive brittleness [20]. Incorporating POSS nanoparticles into PLLA can overcome the above disadvantages [21,22]. In our previous study, a series of octahedral oligomeric silsesquioxanes (POSS-(PLLA)<sub>8</sub>) were prepared to pull into the PLLA tail into the POSS particles and the interfacial interaction between PLLA and POSS. Improve the mechanics and biocompatibility of PLLA [23]. In this chapter, the POSS nanoparticles (POSS-(PLLA)<sub>8</sub>) with 32 PLLA tail chains were compared with (POSS-(PLLA)<sub>32</sub>) nanofibers, and this study was systematically investigated the effects of tail length on the biological properties of nanocomposite fibers.

## 2. Materials and Methods

### 2.1. Materials

Poly(L-lactide) (PLLA,  $M_n = 1 \times 10^5$  g/mol) and L-lactide were purchased from Daigang Biomaterial Co. (Jinan, China). Aminopropyltriethoxysilane ( $\text{NH}_2(\text{CH}_2)_3\text{Si}(\text{OC}_2\text{H}_5)_3$ ,  $\geq 97\%$ ) was supplied by Tianci Silicone Technology Company (Guangzhou, China). Stannous (II) octoate ( $\text{Sn}(\text{Oct})_2$ ) with purity  $\geq 95\%$  was provided by Shanghai Macklin Biochemical Co. Glycidol obtained from sigmaAldrich Co. Other chemicals like chloroform ( $\text{CHCl}_3$ ), hexane, hydro-fluoric acid (HF), dichloromethane (DCM), methanol and ethanol were of analytical-reagent grade and were used without further purification.

### 2.2. Synthetic Preparation Method of POSS-(OH)<sub>32</sub> and POSS-(OH)<sub>8</sub>

#### 2.2.1. PLLA/POSS-OH<sub>8</sub> Hybrid Synthesis Steps:

The synthesis of POSS-(OH)<sub>8</sub> was carried out according to the method we reported previously [23]. In short, it is divided into three steps: In the first step, 0.2 mol of chloropropyltriethoxysilane was weighed using an electronic balance, and concentrated hydrochloric acid (45 mL) and methanol (900 mL) were weighed. The above reagent was added to a round bottom flask at room temperature for magnetic stirring for 35 weeks, and finally a precipitate was obtained. After filtering the reaction liquid, milky white crystals were obtained, which were rinsed 6 times with ultrapure water, and then placed in a dry box for vacuum. Drying gave the desired product octachloropropyl cage silsesquioxane. In the second step, The synthesis of Ag<sub>2</sub>O 2.355 g of AgNO<sub>3</sub> was weighed using an electronic balance, and then dissolved in 10 mL of deionized water, and then 0.56 g of a sodium hydroxide solution was uniformly and slowly dropped, stirred and

shaken, and the precipitate was washed by filtration to finally obtain a product Ag<sub>2</sub>O. In the third part, the octachloropropyl cage silsesquioxane was dissolved in deionized water, then POSS-Cl<sub>8</sub>, 76 mL of each of tetrahydrofuran and ethanol were mixed and added to the round bottom flask, and finally deionized water was added 1 (mL) and Ag<sub>2</sub>O, after stirring, in the dark for 48 h, after which the filtrate in the reaction was evaporated using a rotary evaporator to finally obtain the desired product.

#### 2.2.2. PLLA/POSS-OH<sub>32</sub> Hybrid Synthesis Steps:

According to the previous article, the synthetic POSS-(PLLA)<sub>32</sub> step can be divided into two steps [23]. In the first step, after measuring 2 mol of glycidol, slowly and slowly drop in 1 mol (aminopropyl) triethoxysilane, and carry out ice bath, shake and stir, and react at room temperature for 1h to finally obtain N, N-di (2,3-dihydroxypropyl)-(aminopropyl) triethoxysilane. In the second step, the synthesized N, N-bis (2,3-dihydroxypropyl)-(aminopropyl) triethoxysilane is hydrolytically condensed, and then add the aqueous solution(6.727g) of methanol (200 mL) and HF(3.225%) , reacted at 25 °C for 2h; finally dried in a vacuum at 40 °C to finally obtain PLLA / POSS-OH<sub>32</sub> hybrid.

### 2.3. Synthesis of POSS-(PLLA)<sub>8</sub> and POSS-(PLLA)<sub>32</sub>

According to the research of Liu [23], the synthesis of composite nanomaterials in this paper is based on the molar ratio of lactide to POSS. The ratio of lactide to POSS molar ratio is 1:400. To synthesize POSS-(PLLA)<sub>8</sub> and POSS-(PLLA)<sub>32</sub>.

### 2.4. Preparation of PLLA/POSS Composite Nanofibers

First, weighed two 0.96 g PLLAs with 0.04 g of POSS-(PLLA)<sub>8</sub> and 0.04 g of POSS-(PLLA)<sub>32</sub> dissolved in 9 mL of dichloromethane, one-component PLLA dichloride. The methane solution was used as a control and stirred at 25 °C for 10 h. After the PLLA was completely dissolved, 4 ml of N, N-dimethylformamide (DMF) was added and stirred at 25 °C for 3 h. And then the prepared spinning solution described above was placed in a 20 mL syringe. The electrode of the electrospinning machine is connected to the needle of the syringe, and the aluminum foil is annularly spread on the receiving shaft of the spinning machine. The distance between the needle for controlling the syringe and the receiving aluminum foil was 18 cm, the rotational speed of the receiving shaft was 800 rpm/min, and the electrospinning voltage was 18 KV, and the spinning solution was extruded at a pushing speed of 0.8 ml/h. After the high-voltage electrospinning is completed, the spinning film is taken out and cut, and dried in a dry box.

### 2.5. Characterization

#### 2.5.1. FT-IR Characterization

A small amount of POSS-(OH)<sub>32</sub> and POSS-(OH)<sub>8</sub> samples were uniformly mixed with KBr powder, and then the above powder was sufficiently ground using a mortar and then pressed, and then placed in a Fourier infrared spectrometer for measurement. The resolution used is 4

cm<sup>-1</sup> and the scanning range is 4000-500 cm<sup>-1</sup>.

For the infrared test method of PLLA/POSS-(OH)<sub>8</sub>, PLLA/POSS-(OH)<sub>32</sub> composite fiber prepared by electrospinning: the prepared nanofiber is fixed on a zinc crystal plate, and then placed in the path of infrared laser to exam. The resolution used is 4 cm<sup>-1</sup> and the scanning range is 4000-500 cm<sup>-1</sup>.

### 2.5.2. F-SEM Characterization of Surface Morphology of Nanofiber Composite Films

The three composite nanofiber membranes which were dried were respectively cut into squares having a size of about 0.5×0.5 cm. The three kinds of composite fibers were adhered to a special copper table with conductive adhesive, and the gold plating film was sprayed by ion sputtering vacuum coating for about 45 s, the thickness of the gold film was about 0.5-10 nm, and finally the composite nanofiber after gold spraying. Put into the field and scan the inside of the scanning electron microscope and vacuum, observe the surface morphology of different fibers and take pictures. The accelerating voltage used is 20 KV. At the same time, Image J software was used to analyze the surface topography of the fiber and measure the diameter of the composite fiber (measured 50 per photo).

### 2.5.3. Dynamic Thermomechanical Analysis (DMA)

Three kinds of nanofiber spinning films of the same thickness were selected, and they were cut into a rectangular shape of 50 mm and a width of 40 mm. The uniaxial tensile test was performed on the spinning film by a tensile machine of a load unit of 10000 N at room temperature. The tensile test was carried out at a tensile speed of 5 mm/min. The ultimate tensile length was 30 mm. Ten parallel samples were tested for each group of nanofibers. Finally, the average value was calculated and the stress-strain curves, tensile strengths and modulus of elasticity were calculated.

### 2.5.4. Water Absorption Test

Three composite nanofibers (PLLA, PLLA/POSS-(OH)<sub>8</sub>, PLLA/POSS-(OH)<sub>32</sub>) were taken and cut into squares of 2.0 x 2.0 cm. The composite fiber was accurately weighed using an analytical balance, and its mass was recorded as G<sub>1</sub>. Then, the composite fiber sample was immersed in a container filled with ionized water, and the fiber sample was taken out every 2 hours, and the moisture of the surface of the fiber membrane was quickly absorbed by the water-absorbing filter paper. Its quality is recorded as G<sub>2</sub>. Formula (1) for calculating the water absorption of composite fibers:

$$R = \frac{G_2 - G_1}{G_1} \times 100\% \quad (1)$$

### 2.5.5. Evaluation of Cell Compatibility of Composite Nanofibers

HUVECs cells were incubated in a cell culture incubator, and when the cell spreading area exceeded 90% of the bottom of the flask, digestion was performed using 0.25% EDTA (trypsin). On the other hand, three composite

nanofibers (PLLA, PLLA/POSS-(OH)<sub>8</sub>, PLLA/POSS-(OH)<sub>32</sub>) were cut into circles of approximately 0.8 cm in diameter (four sets of parallel samples were set for each group). After placing in a 24-well plate, 1.5 ml of 75% ethanol was added to each well containing the sample, and the cells were sealed for 4 hours, and the ethanol solution was aspirated, washed three times with PBS, and then sterilized by using an ultraviolet lamp for 40 minutes. The digested HUVECs cells were collected, and 1 ml of the cell culture medium and 2×10<sup>5</sup> cells/well were seeded onto the surface of three nanofibers. Finally, the 24-well plate after seeding the cells is placed in a cell culture incubator for incubation, and fresh cell culture medium is changed every other day.

### 2.5.6. Characterization of Cellular Activity of Composite Nanofibers

In this article, the Cell Counting Kit-8 (CCK-8 kit) reagent was used to characterize the effect of fiber samples on the activity of HUVECs. CCK-8 is widely used in the detection of cell activity and value-added. Compared with conventional MTT assay, it has the advantages of simple operation, low risk and reliable repeatability.

After 1, 3, 5, and 7 days after seeding the cells, the medium in the wells of the well plate samples was separately aspirated, and 1 ml of CCK-8 mother liquor was added to each well (the ratio of the cell culture medium of CCK-8 was 1:9). The cells on the surface of the sample were completely submerged, and then the 24-well plate was implanted in a cell culture incubator for 1 h. The mother liquor after incubation was then aspirated using a pipette, dispensed in a 96-well plate at 100 μL/well, and shaken for 10 min using a shaker. The absorbance at 450 nm was selected in a microplate reader to determine the absorbance value of each sample surface. The control group in this study was a blank culture plate, and each group was measured in parallel three times and averaged.

### 2.5.7. Cell Morphology Observation

After the cells are seeded onto the surface of the material, the cells on the surface of the material are treated. The culture plate was taken out in a cell culture incubator, the upper culture medium was aspirated using a pipette, and the cells on the surface of the material were washed three times with a PBS buffer solution, and then fixed with 4% paraformaldehyde for 1 h, and then the fixing solution was aspirated. After PBS was slowly washed for 3 times, the cells were dehydrated with 50%, 60%, 70%, 80%, 90%, 100% ethanol, respectively, for 20 min each time. The cells dehydrated by the alcohol gradient were transferred to a dry box for drying. The dried cells were sampled, sprayed with gold, and observed under a scanning electron microscope.

### 2.5.8. Laser Confocal Microscopy

For immunofluorescence analysis, cells were fixed with 4 % paraformaldehyde and permeabilized by 0.1 % Triton X-100. Then 1 % bovine serum albumin (BSA, Sigma) were used to block the unspecific binding sites. Actin filaments were stained with rhodamine-conjugated

phalloidin (R415, Life) and nucleus were stained with 4',6-diamidino-2-phenylindole (DAPI, D357, Life) in the dark. After immunostaining, the confocal laser scanning microscopy (CLSM, Carl Zeiss LSM 880 META, Jena, Germany) was performed.

### 3. Statistical Analysis

In this article, the average value  $\pm$  standard deviation (SD) of all experimental statistics was calculated using SPSS 19.0 software. All tests were set up in three parallel samples. The single factor variable analysis method (ANOVA) was used to evaluate the statistical difference of the results. In the histogram, \* indicates  $p < 0.05$ , and \*\* indicates  $p < 0.01$ . The smaller the p value, the more \* corresponding to the more significant statistical difference between the two sets of data.

## 4. Results and Discussion

### 4.1. Infrared Analysis of Composites

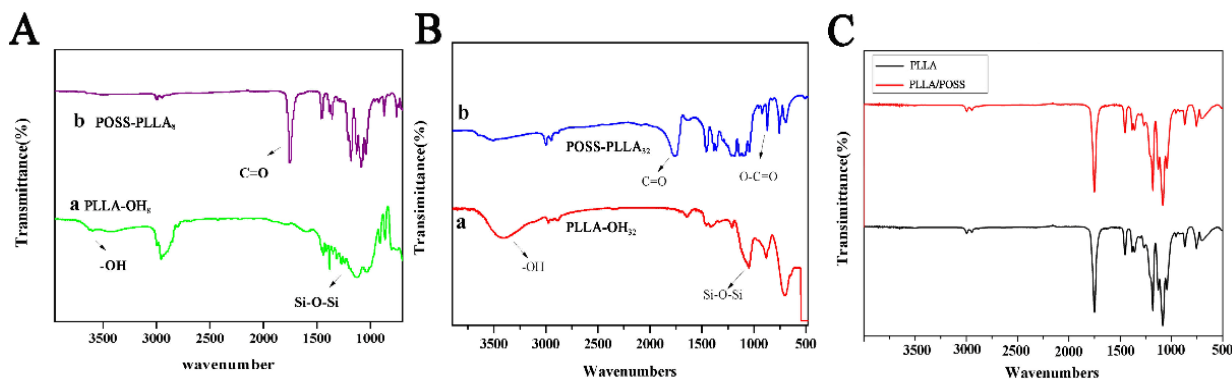


**Figure 1.** FT-IR graph of serial Polyhedral Oligomeric Silsesquioxane: A, Poly(lactic Acid) /Polyhedral Oligomeric Silsesquioxane-OH<sub>8</sub>; B, Poly(lactic Acid) / Polyhedral Oligomeric Silsesquioxane-OH<sub>32</sub>; C, FT-IR graph of serial fiber membrane.

### 4.2. Basic Characteristics of Composite Nanofibers

Figure 2A and D, B and E are FESEM photographs of PLLA and PLLA/POSS-(PLLA)<sub>32</sub> 4% composite fibers, respectively. It can be seen from the figure that neither fiber has a porous structure, and the diameters of the two fibers are about 350 nm and 450 nm, the size is basically close. From the appearance structure analysis PLLA and PLLA/POSS-(PLLA)<sub>32</sub> 4% composite fiber, pure PLLA nanofiber membrane has many defects such as cracks, which may be due to the stretching of PLLA under the action of electric field force during electrospinning. Because of its poor mechanical strength, it is prone to brittle fracture, so that many cracks appear on its surface. The PLLA/POSS-(PLLA)<sub>32</sub> 4% composite fiber exhibits a ribbon-like structure. Probably the mechanical properties of PLLA doped with POSS-(PLLA)<sub>32</sub> have led to some improvement. The POSS nanoparticles in the PLLA

matrix act as heterogeneous nucleating agents and accelerate the crystallization of the PLLA chain [23] and accelerate electrospinning. The phases in the process are separated to form a strip-like appearance structure. Figure 2 C and F is a FESEM photograph of PLLA/POSS-(PLLA)<sub>8</sub> 4% composite fiber. From the figure, It can be seen that the composite fiber has a regular distribution and interconnected pore structure. The average diameter of the composite fiber is 273  $\mu\text{m}$ , and the average diameter of the pores is 2.53 nm. Significant pores appear in the fiber, which may be a significant improvement in the mechanical properties of PLLA doped with PLLA/POSS-(PLLA)<sub>8</sub>, and POSS has a hydrophobic effect, which increases the hydrophobicity of the system, promotes the phase of the system separation, and makes holes appear from the surface of the fiber.

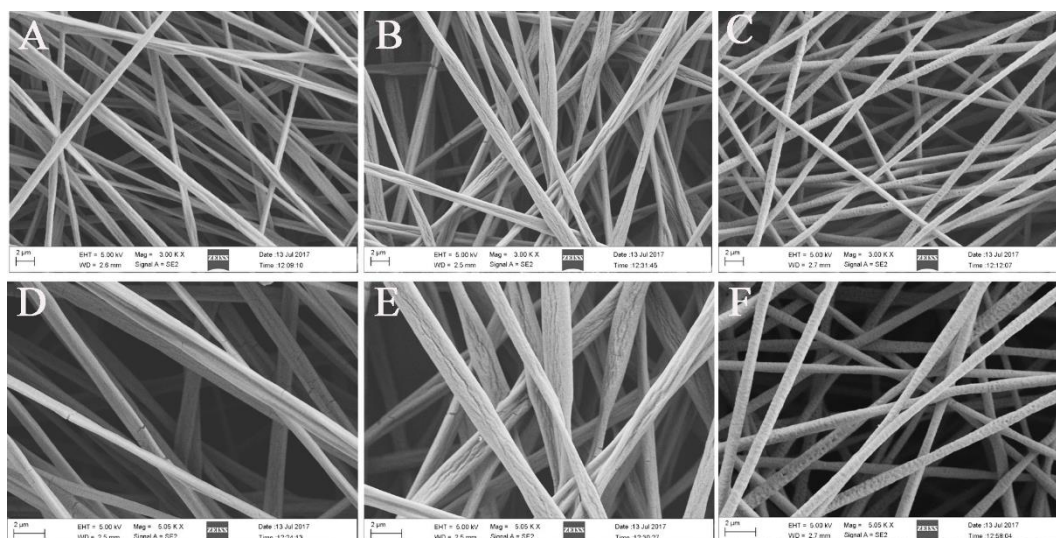


**Figure 2.** SEM images and nanofiber distribution graphs of neat PLLA nanofiber membranes (AD) pure PLLA, (BE) PLLA/POSS-(PLLA)<sub>32</sub>, (BE) PLLA/POSS-(PLLA)<sub>8</sub> of 4%.

### 4.3. Hydrophilicity of Composite Nanofibers

The measurement of the water absorption of the composite fiber membrane is also an important component of the hydrophilicity of the composite nanofiber. In order to visually reflect the hydrophilicity inside the composite fiber, further detection of water absorption is indispensable. Figure 3 shows the water absorption of the three composite fibers after soaking for 4, 8, 12, 16 and 20 h. As can be seen from the figure, with the incorporation of POSS-(PLLA)<sub>8</sub>, the greater the water absorption of the composite nanofibers, the better the hydrophilic properties. And it was found that the water absorption of the three composite fibers did not change greatly after 12 hours of infiltration, because both of them had reached the state of saturated water absorption. For the PLLA/POSS-(PLLA)<sub>8</sub> composite fiber, the saturated water absorption state has been reached after 8h, indicating that the water absorption speed is faster, and it also reflects that the incorporation of POSS-(PLLA)<sub>8</sub> can significantly improve the hydrophilicity of PLLA nanofibers.

The porosity of a nanofiber refers to the ratio of the pore volume of the composite fiber to the total volume of the composite fiber in a natural state. Which can be characterized by its gas permeability and moisture permeability, it reflects the cytocompatibility affecting the composite fiber to a certain extent. Based on the FESEM image of the above fiber (Figure 3), the composite fiber membrane prepared by the electrospinning technique has a unique network structure, and its microscopic morphology and densely packed pore structure are similar to those of the extracellular matrix.

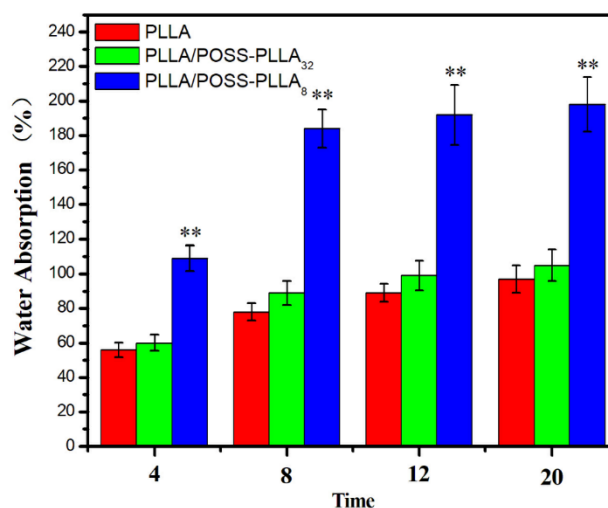


**Figure 3.** Water absorption of nanofibers after PLLA is combined with different types of POSS-PLLA<sub>n</sub>.

### 4.4. Mechanical Properties of Composite Nanofibers

The mechanical properties of biological materials are critical in tissue engineering applications. The mechanical properties of materials can affect the spreading and adhesion of cells, so good mechanical properties are essential. The mechanical properties of pure PLLA and PLLA and different types of POSS-PLLA<sub>n</sub> composite nanofiber membranes were characterized by tensile experiments. Figure 4 shows the stress-strain curves of the materials.

Comparing the mechanical changes of POSS-PLLA<sub>8</sub> and POSS-PLLA<sub>32</sub> nanoparticles to PLLA materials, POSS-PLLA<sub>8</sub> nanoparticles can greatly improve the toughness of PLLA, and the mechanical strength of composite fibers is also greatly improved. The main reason for this difference is that POSS-PLLA<sub>32</sub> composite nanoparticles have 32 tail chains, and their tail chain length is much smaller than POSS-PLLA<sub>8</sub> nanoparticles, so they have large steric hindrance. When stressed, POSS-PLLA<sub>32</sub> particles cannot enter the folded crystal region and are less mechanically dissipated. POSS-PLLA<sub>32</sub>

nanoparticles have fewer tail chains and longer tail lengths. When subjected to tensile force, it can withstand less steric hindrance, and has better interfacial compatibility after the composite PLLA matrix material, so the elongation at break increases greatly.

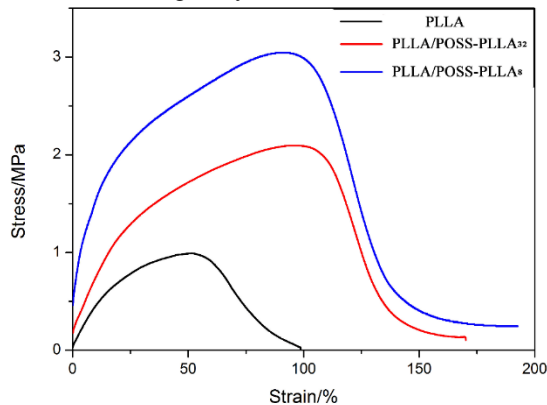


**Figure 4.** Stress-strain curves of composite nanofiber membranes.

#### 4.5. In Vitro Biological Evaluation of Composite Nanofibers

In this article, the CCK-8 kit was used to characterize the cell viability on the surface of composite fiber membranes, and the growth state and spreading morphology of HUVECs cells on composite fibers were observed using confocal microscopy (CLSM) and scanning electron microscopy (SEM). Figure 5 shows the results of activity experiments of HUVECs on the surface of three kinds of nanofibers for 1, 3, and 5 days. As shown in the Figure 5, the proliferation of cells on the nanofibers increases with the prolongation of the culture time. After 3 and 5 days of culture, the cells proliferated on the three groups of fibers significantly better than the control group, because PLLA has better biocompatibility and the three fibers provide a larger spreading area for the cells. Among them, PLLA/POSS-PLLA<sub>8</sub> composite nanofiber membrane has the best proliferation effect on HUVECs, because porous composite nanofibers are more conducive

to the extension of cellular pseudopods, thereby promoting cell adhesion and growth.

The experimental results of the above composite nanomechanical properties and hydrophilicity show that the doping of POSS-PLLA<sub>8</sub> can significantly improve the cell viability of PLLA matrix materials.

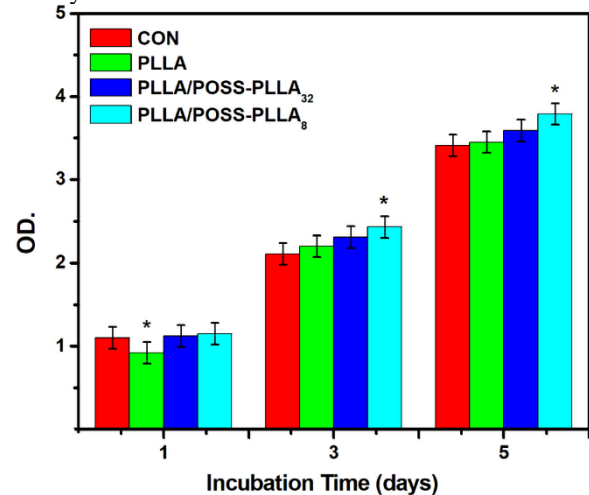


**Figure 5.** The CCK-8 assay of HUVECs cells cultured on composite nanofiber membranes.

Figure 6 is a FSEM photograph of HUVECs cultured on pure PLLA and PLLA/POSS-PLLA<sub>n</sub> fiber composite membrane for 3 days. It can be seen from Figure 5 that the growth state and spreading of HUVECs cells on the three nanofiber membranes are better. For the PLLA/POSS-PLLA<sub>8</sub> fiber composite membrane, HUVECs cells have the largest area of spreading and aggregation on them, and the cells aggregate into a very flat “membrane” structure, which does not appear on the other two groups of fibers. In short, endothelial cells accumulate on the surface of the composite fibers, causing their endothelialization on the surface of the material, so that the new blood vessels are not easily aggregated and damaged, thereby effectively preventing the development and occurrence of restenosis of the blood vessels.

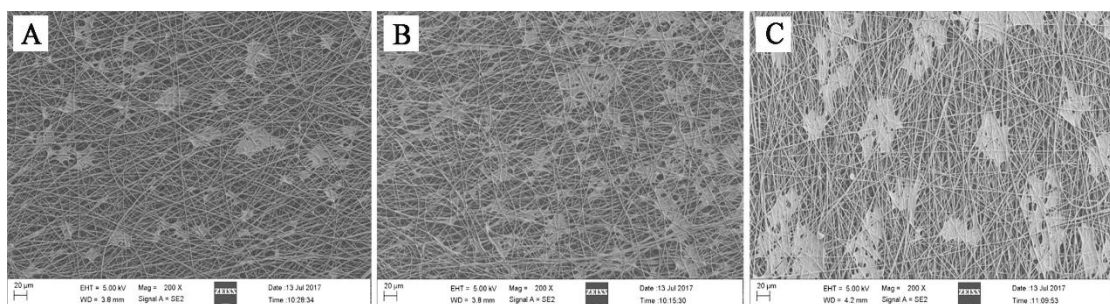


**Figure 6.** F-SEM micrographs of HUVECs cultured on the nanofiber of neat PLLA nanofiber membranes (A), PLLA/POSS-PLLA<sub>32</sub> (B) and PLLA/POSS-PLLA<sub>8</sub> (C).

The cytoskeleton is a network of protein fibers, which is mainly found in the whole cytoplasm. The cytoskeleton can be divided into microtubules, microfilaments and intermediate fibers, which are important for cell proliferation and spreading. Focal adhesion refers to the physical connection between cells and extracellular matrices. It plays a significant role in the physiological activities of organisms because they regulate cell adhesion

and mechanical sensing, and signals that control the signal of the cell growth, movement and differentiation.

The adhesion and morphology of HUVECs cells on the surface of three fibers were observed using a laser confocal microscope (Figure 7). In the Figure 7, DAPI stains the nucleus in blue, and Rhodamine-Phalloidin dyes actin in red, and the plaque is stained green. As can be seen from the figure, the number of cells on the nanofiber membrane

increases as the culture time increases. At the same time, it can be seen that the cells and the cells exhibit a state of aggregation and growth, and the aggregation area increases with time. It can be seen from the C-F that the aggregate area is expanding. It can be seen from the figure that the morphology of HUVECs on PLLA and PLLA/POSS-PLLA<sub>32</sub> nanofiber membranes is similar, and small clusters are formed between cells and cells, and this small mass increases and get bigger with time goes. However, the cell agglomerate area formed on the PLLA/POSS-PLLA<sub>8</sub> composite nanofibers is the largest.

Based on the above results, different nanofibers have a greater impact on the formation of HUVECs cell clumps. PLLA/POSS-PLLA<sub>8</sub> composite porous nanofibers have

the largest number of cells aggregated, the largest spreading area, and the formation of larger cell clusters. The number of cells and the spread area are minimal on pure PLLA nanofibers. PLLA/POSS-PLLA<sub>8</sub> composite porous nanofibers promote cell-to-cell linkage and increase their effects on cell proliferation. This porous feature also facilitates the exclusion of the adhesion of the fibers themselves to the cells, and better illustrates the effect of the porous structure on HUVECs. At the same time, it can be seen that the spread of cells on the nanofibers without porous structure and the size of the agglomerates are not much different, indicating that the introduction of organic-inorganic POSS-PLLA nanoparticles has little effect on the whole cell.

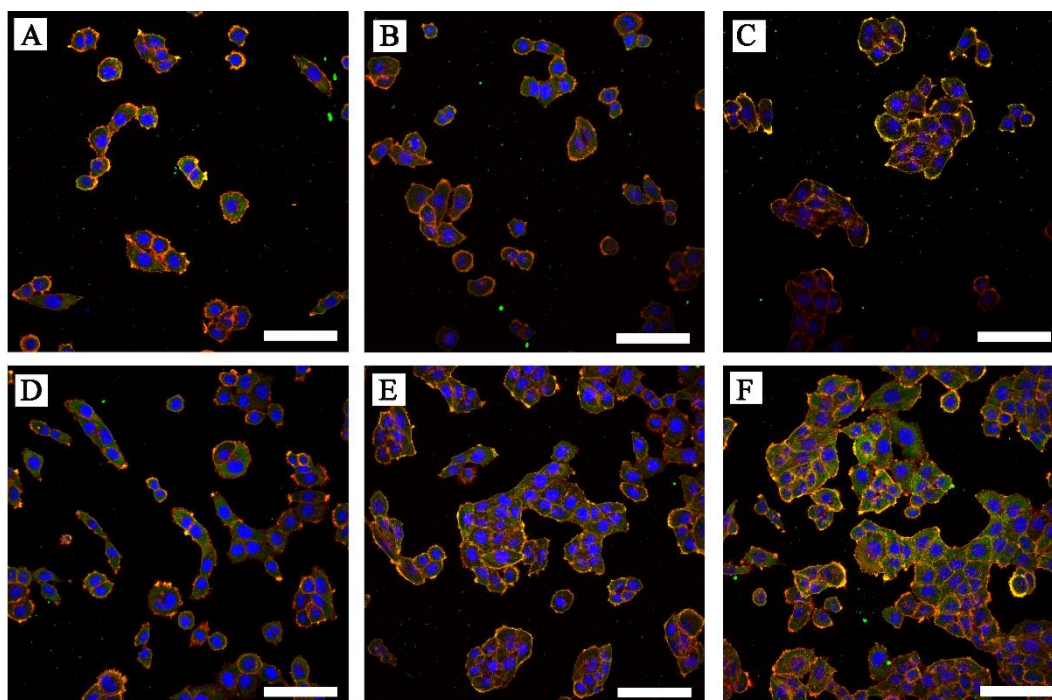


**Figure 7.** Morphology of HUVECs cultured on nanocomposite fiber surfaces. Images of HUVECs stained for actin (red), vinculin (green) and nuclei (DAPI, blue) and cultured for 3 and 5 days on PLLA (AD), PLLA/POSS-PLLA<sub>32</sub> (BE) and PLLA/POSS-PLLA<sub>8</sub> (CF) nanofibers.

## 5. Conclusions

In this article, eight-arm (3-hydroxypropyl) cage silsesquioxane was prepared by condensation hydrolysis method. Based on this, by controlling the ratio of POSS to lactide, synthesize the POSS-(PLLA)<sub>32</sub> and POSS-(PLLA)<sub>8</sub> nanoparticles with different PLLA arm lengths.

Two kinds of nanoparticles, POSS-PLLA<sub>8</sub> and POSS-PLLA<sub>32</sub>, were composited in PLLA, and the PLLA/POSS-PLLA<sub>n</sub> nanofiber composite film was successfully fabricated by electrospinning. The field morphology of the composite fiber was characterized by field emission scanning electron microscopy. The fiber of POSS-(PLLA)<sub>8</sub> composite nanofiber has a relatively good uniform distribution and a regular porous structure with a diameter of 300-700 nm. From the FESEM chart, the POSS-(PLLA)<sub>8</sub> nanoparticles have good dispersibility, and no serious agglomeration occurs on the surface of the composite fiber. Compared with pure PLLA nanofibers,

the adjunction of POSS-PLLA<sub>8</sub> introduce a large number of relatively regular and small size wafers, which form the most compact and largest number of crystals and improve the thermal stability and hydrophilic properties of PLLA/(POSS-(PLLA)<sub>8</sub>) composite nanofibers. The (POSS-(PLLA)<sub>8</sub>) nanoparticles are introduced into the PLLA matrix material, and the nanoparticles act as a heterogeneous nucleating agent, which greatly increases the crystallinity of the system, and the composite material has a smaller size and a more regular crystal form. The strength of the composite material has been greatly improved. On the other hand, the incorporation of (POSS-(PLLA)<sub>8</sub>) nanoparticles can effectively promote the interaction of the interface and improve the interfacial compatibility. In addition, PLLA/(POSS-(PLLA)<sub>8</sub>) composite porous nanofibers can promote cell proliferation, spreading and adhesion, and have good biocompatibility.

## Acknowledgment

The authors appreciate the help from Department of Materials Science and Engineering, Jinan University, Guangzhou, China.

## References

- [1] Sharma R.; Sharma S.; Dutta S.; Zboril R.; Gawande M.B. Silica-nanosphere-based organic-inorganic hybrid nanomaterials: synthesis, functionalization and applications in catalysis. *Green Chemistry*, **2015**, 17: 3207-30.
- [2] Zhao H.R.; Zhang T.; Qi R.R.; Dai J.X.; Liu S.; Fei T.; et al. Development of solution processible organic-inorganic hybrid materials with core-shell framework for humidity monitoring. *Sens. Actuator. B-Chem.*, **2018**, 255: 2878-85.
- [3] Zheng L.; Farris R.J.; Coughlin E.B. Novel polyolefin nanocomposites: Synthesis and characterizations of metallocene-catalyzed polyolefin polyhedral oligomeric silsesquioxane copolymers. *Macromolecules*, **2001**, 34: 8034-8039.
- [4] Zhou H.; Ye Q.; Xu J.W. Polyhedral oligomeric silsesquioxane-based hybrid materials and their applications. *Mat. Chem. Front.*, **2017**, 1: 212-230.
- [5] Tanaka K.; Chujo Y. Unique properties of amphiphilic POSS and their applications. *Polym J.*, 2013, 45: 247-254.
- [6] Wang F.; Lu X.; He C. Some recent developments of polyhedral oligomeric silsesquioxane (POSS)-based polymeric materials. *Journal of Materials Chemistry*, 2011, 21: 2775-2782.
- [7] Janowski B.; Pielichowski K. Nano-hybrid polymers containing polyhedral oligosilsesquioxanes (POSS), 2008.
- [8] Kaiqiang Z.; Bo L.; Yunhui Z.; Hui L.; Xiaoyan Y. Functional POSS-containing polymers and their applications. *Progress in Chemistry*, **2014**, 26: 394-402.
- [9] Michałowski S.; Hebda E.; Pielichowski K. Thermal stability and flammability of polyurethane foams chemically reinforced with POSS. *J. Therm. Anal. Calorim.*, **2017**, 130: 155-63.
- [10] Li L.; Liu H. Facile construction of hybrid polystyrene with a string of lantern shape from monovinyl-substituted POSS and commercial polystyrene via Friedel-Crafts reaction and its properties. *RSC Advances*, **2014**, 4: 46710-46717.
- [11] Sun M.; Yin W.; Dong X.; Yang W.; Zhao Y.; Yin M. Fluorescent supramolecular micelles for imaging-guided cancer therapy. *Nanoscale*, **2016**, 8: 5302-5312.
- [12] Yang Q.; Tan L.; He C.; Liu B.; Xu Y.; Zhu Z.; et al. Redox-responsive micelles self-assembled from dynamic covalent block copolymers for intracellular drug delivery. *Acta biomaterialia*, **2015**, 17: 193-200.
- [13] Shan X.; Li F.; Liu C.; Gao Q. Electrospinning of chitosan/poly (lactic acid) nanofibers: the favorable effect of nonionic surfactant. *J. Appl. Polym. Sci.*, **2014**, 131.
- [14] Zeng S.; Cui Z.; Yang Z.; Si J.; Wang Q.; Wang X.; et al. Characterization of highly interconnected porous poly (lactic acid) and chitosan-coated poly (lactic acid) scaffold fabricated by vacuum-assisted resin transfer molding and particle leaching. *Journal of Materials Science*, **2016**, 51: 9958-9970.
- [15] Zhang H.; Mao X.; Du Z.; Jiang W.; Han X.; Zhao D.; et al. Three dimensional printed macroporous polylactic acid/hydroxyapatite composite scaffolds for promoting bone formation in a critical-size rat calvarial defect model. *Science and Technology of advanced Materials*, **2016**, 17: 136-148.
- [16] Pal J.; Kankariya N.; Sanwaria S.; Nandan B.; Srivastava R.K. Control on molecular weight reduction of poly ( $\epsilon$ -caprolactone) during melt spinning—A way to produce high strength biodegradable fibers. *Materials Science and Engineering: C*, **2013**, 33: 4213-4220.
- [17] Ramot Y.; Haim-Zada M.; Domb A.J.; Nyska A. Biocompatibility and safety of PLA and its copolymers. *Advanced drug delivery reviews*, **2016**, 107: 153-162.
- [18] Liu K.; Wang N.; Wang W.; Shi L.; Li H.; Guo F.; et al. A bio-inspired high strength three-layer nanofiber vascular graft with structure guided cell growth. *Journal of Materials Chemistry B*, **2017**, 5: 3758-3764.
- [19] Zhu C.; Ma X.; Xian L.; Zhou Y.; Fan D. Characterization of a co-electrospun scaffold of HLC/CS/PLA for vascular tissue engineering. *Bio-medical materials and engineering*, **2014**, 24: 1999-2005.
- [20] Davachi S.M.; Bakhtiari S.; Pouresmaeel-Selakjani P.; Mohammadi-Rovshandeh J; Kaffashi B.; Davoodi S.; et al. Investigating the effect of treated rice straw in PLLA/starch composite: mechanical, thermal, rheological, and morphological study. *Advances in Polymer Technology*, **2018**, 37: 5-16.
- [21] Han D.; Wen T.J.; Han G.; Deng Y.Y.; Deng Y.; Zhang Q.; et al. Synthesis of Janus POSS star polymer and exploring its compatibilization behavior for PLLA/PCL polymer blends. *Polymer*, **2018**, 136: 84-91.
- [22] Tamburaci S.; Tihminlioglu F. Novel poss reinforced chitosan composite membranes for guided bone tissue regeneration. *Journal of Materials Science: Materials in Medicine*, **2018**, 29: 1.
- [23] Liu Z.; Hu D.; Huang L.; Li W.; Tian J.; Lu L.; et al. Simultaneous improvement in toughness, strength and biocompatibility of poly (lactic acid) with polyhedral oligomeric silsesquioxane. *Chemical Engineering Journal*, **2018**, 346: 649-661.